Indirect effect of hydrogen bonds on the magnetic coupling on MnIJIII) dinuclear compounds†

J. M. Pagès,[a] L. Escriche-Tur, [a] M. Font-Bardia, [bc] G. Aullón [*ad] and M. Corbella [*ae]

a Departament de Química Inorgànica i Orgànica (Secció Química Inorgànica), Facultat de Química, Universitat de Barcelona, Martí i Franquès 1, 08028 Barcelona, Spain**. E-mail: gabriel.aullon@qi.ub.es, montse.corbella@qi.ub.es**

b Departament de Mineralogia, Petrologia i Geologia Aplicada, Facultat de Ciències de la Terra, Universitat de Barcelona, Martí i Franquès s/n, 08028 Barcelona, Spain

c Unitat de Difracció de RX, Centres Científics i Tecnològics de la Universitat de Barcelona (CCiTUB), Universitat de Barcelona, Solé i Sabarís 1-3, 08028-Barcelona, Spain

d Institut de Química Teòrica i Computacional (IQTCUB), Universitat de Barcelona, Martí i Franquès 1, 08028 Barcelona, Spain

e Institut de Nanociència i Nanotecnologia (IN2UB), Universitat de Barcelona, Martí i Franquès 1, 08028 Barcelona, Spain

ABSTRACT:

The MnIJIII) dinuclear compounds [{MnIJbpy)IJH2O)}IJμ-2,6-Cl2C6H3COO)2IJμ-O){MnIJbpy)IJX)}]X, where X = ClO4 (1) or X = NO3 (2), were synthesised and characterised by X-ray diffraction spectroscopy. In both cases there were hydrogen bond interactions between the aqua ligand and counteranions, but with different connectivity patterns. For compound 1, the interactions connected two dinuclear complexes through two perchlorate counteranions to generate a tetranuclear unit. For compound 2, the hydrogen bond was "intramolecular" between the cationic complex, nitrate counteranion and crystallization water (Mn–LW···NO3 −···H2O···LN–Mn). This unusual interaction was responsible for the perfect orthogonality of the coordination octahedra on the dinuclear entity and noticeable elongation of these polyedra. Both compounds showed antiferromagnetic coupling, which was unusually strong for compound 2 with a nitrate anion (J = −9.2 and −27.3 cm−1 for 1 and 2, respectively) (H = −J·S1·S2). The effect of the counteranion (X) on the magnetic interaction was analysed by density functional theory studies. For both compounds, hydrogen bonds between the aqua ligand and counteranions weakened the antiferromagnetic interaction. Moreover, for 2, replacement of the counteranion nitrate with other groups had a significant effect on the magnetic interaction.

INTRODUCTION

Interest in MnIJIII) dinuclear compounds with a [Mn2IJμ-O)IJμ-R′COO)2]2+ core is based on the possibility of obtaining compounds with two spin ground states: S = 0 or S = 4. Several magneto-structural correlations have been reported for acetate and benzoate derivatives as carboxylate bridging ligands. Systems with major "flexibility" are hexacoordinated MnIJIII) ions achieved by diimine chelate ligands, together one oxo and two bridging benzoate derivatives, [{MnLIJNN)}IJμ-O)IJμ-RC6H4COO)2{MnL′(NN)}]X2−n. The X− anion (N3−, NO3− orClO4−)1–12 can be incorporated as a ligand in the sixth position. Consequently, three classes of systems have been obtained: dicationic complexes with neutral ligands such as H2O or EtOH remaining both X as counteranions; neutral complexes when these anions acts as ligands; monocationic complexes when the two metallic ions present different charged ligands as a neutral and an anion.

The nature of the monodentate ligand (L, L′) is one of the most influential factors for distortion of the coordination octahedral around MnIJIII) ions (compression or elongation)2,3 and in the orientation of the distortion axes.1,4 These facts are related to the magnetic interaction and spin ground state. From the 28 compounds of this type characterized magnetically and structurally, only two have shown compressed octahedral in the oxo bridge direction, resulting in ferromagnetic interaction in the two cases with ground spin state S = 4. These compounds have L = L′ = N3,1 and L = H2O and L′ = NO3,4 respectively.

Despite these two exceptions, the remainder of the compounds have distortion axes in the monodentate ligand direction, and the octahedra are elongated or show rhombic distortion. The degree of elongation/rhombicity is one of the main parameters affecting the magnetic interaction.

Nevertheless, other parameters are also revealed to modify magnetic coupling, such as the relative disposition of the coordination octahedra (L–Mn···Mn–L′ torsion angle), the Mn–O–Mn angle, and the twist of the aromatic ring of the benzoate derivative bridge.2,3

The coordination of nitrate or perchlorate anions has a significant influence on the degree of elongation of the coordination octahedra.3 Moreover, if there is at least one aqua ligand, hydrogen bonds between this ligand and the counteranion are observed. This interaction could be limited to the aqua ligand of the cationic complex (LW) and the counteranion (X−) or extended connecting neighbour dinuclear entities.

For the nitrate compounds, most of them form one-dimensional systems due to the hydrogen bonds connecting with dinuclear entities directly, i.e., LW···LN (aqua and nitrate as ligands) or through the counteranion LW···NO3 −···LW.2–4,6,9–12 Moreover, they predominantly show a ground state of S = 4 for the dinuclear entity.

For the perchlorate compounds, only half of them result in one-dimensional systems by hydrogen bonding, as in the preceding case, both types are found (LW···ClO4 −···LW and LW···LCl).3,6,7,10,11 Nevertheless, other cases present these interactions by connecting only two dinuclear entities to make a tetranuclear unit.2,4,6 From the magnetic viewpoint, most of these compounds show a spin ground state

S = 0. Only few of them with ground spin state S = 4 have hydrogen bonds between dinuclear entities to generate a one-dimensional system.

From the first study of the magnetic coupling mediated by hydrogen bonds in mononuclear complexes of CuIJII) ions,13 some other cases of mononuclear and polynuclear compounds with intermolecular magnetic interaction have been reported.14–23 Moreover, in at least one case, an intramolecular hydrogen bond that provides a new way for magnetic coupling has been reported.24 There are also two clusters with SMM properties that have been affected by magnetic interaction through hydrogen bonds between the clusters.25,26

In the present study, we report two newMnIJIII) dinuclear compounds with a dichlorobenzoate bridge, [{MnIJbpy)IJH2O)}IJμ-2,6-Cl2C6H3COO)2IJμ-O){MnIJbpy)IJX)}]X, where X = ClO4 − (1) or NO3 − (2). We wished to observe the influence of the steric hindrance and electronic effect of the two chloro substituents of the benzoate bridge on structural parameters and magnetic properties. Moreover, the network of hydrogen bonds generated by the counteranions and their influence on magnetic behaviour was analysed. To clarify the role of the hydrogen bonds between the counteranion and cationic complexes, density functional theory (DFT) studies were carried out for both compounds.

RESULTS AND DISCUSSION

Synthesis

MnIJIII) dinuclear compounds were obtained by a comproportionation reaction between MnX2 (X = ClO4 (1), NO3 (2)) and Bu4NMnO4 in the presence of the carboxylic acid 2,6-Cl2C6H3COOH and 2,2′-bipyridine (bpy). Compound 1 [{MnIJbpy)IJH2O)}IJμ-2,6-Cl2C6H3COO)2IJμ-O){MnIJbpy)-IJClO4)}]ClO4 crystallised by slow diffusion of n-hexane into an CH3CN solution of 1 layered with CH2Cl2. Compound 2·H2O ·CH3CN [{MnIJbpy)IJH2O)}IJμ-2,6-Cl2C6H3COO)2IJμ-O){MnIJbpy)-IJNO3)}]NO3·H2O·CH3CN crystallised directly from the acetonitrile mother liquor by slow evaporation at room temperature.

The infrared spectra of these compounds showed characteristic bands of the carboxylate ligand at ∼1600 cm−1 and 1390 cm−1 corresponding to asymmetric (νa) and symmetric (νs) vibrations, respectively. The value of Δν = νaIJCOO) −νsIJCOO) ∼210 cm−1 is indicative of carboxylate ligands coordinated in bidentate bridging mode (μ1,3).27 In addition, compound 1 showed the characteristic band of ClO4 − at ∼1100 cm−1. For compound 2, NO3 − showed a very strong band at ∼1385 cm−1; this band overlapped with the νs of the carboxylate group and therefore it was not possible to distinguish between coordinated and non-coordinated ions. The bipyridine ligand showed three characteristic bands in the 1500–1445 cm−1 region and the Mn–Ob–Mn group usually displayed a band at ∼730 cm−1.

Description of the structures

The crystal structures of compounds 1 and 2·CH3CN·H2O showed a dinuclear cationic complex [{MnIJbpy)IJH2O)}IJμ-2,6-Cl2C6H3COO)2IJμ-O){MnIJbpy)IJX)}]+ and non-coordinated perchlorate or nitrate counteranions (X). The cationic complexes of these compounds are shown in Fig. 1 and 2. In both compounds, the two MnIJIII) ions were bridged by one oxo and two 2,6-Cl2C6H3COO− ligands. Each manganese ion was chelated by a 2,2′-bipyridine (bpy) ligand, and hexacoordination was completed by a monodentate ligand, which was a water molecule in one manganese atom and X anion in the other one. The structural parameters of 1 and 2 were in agreement with those reported for analogous compounds with the same [Mn2IJμ-O)IJμ-R′COO)2]2+ core.1–12 Select interatomic distances and angles are shown in Tables 1 and 2.

The Mn···Mn distance was ∼3.16 Å and Mn–Ob–Mn angle was ∼124°. The Mn–O bond length of the oxo bridge was ∼1.79 Å and Mn–N distance was ∼2.06 Å. The carboxylate bridging ligands were coordinated in a syn–syn conformation. One of the oxygen atoms was placed trans to the monodentate ligand with a Mn–Ot distance of ∼2.15 Å for 1 and ∼2.21 Å for 2, whereas the other oxygen atom was placed in the cis position with a shorter Mn–Oc distance (∼1.97 Å) and was similar for both compounds. The Mn–OW distance for the aqua ligand was similar in both compounds (∼2.23 Å), whereas Mn–OL distance involving the anion as a monodentate ligand (ON and OCl atoms, respectively), was larger for ClO4− than for NO3− (2.33 and 2.21 Å for 1 and 2, respectively).

The carboxylate group and aromatic ring of the benzoate derivative bridge was not coplanar; the twist angle ω(O–Ccarb–Car–Car) was ∼74° for both compounds, probably due to the hindrance of chlorine atoms in the aromatic ring. No significant difference was observed between 1 and 2, despite the dissimilar shape and volume of the monodentate ligand on Mn2. The relative disposition of the coordination octahedral could be analysed by the torsion angle between the elongation axes, τ(L–Mn···Mn–L). This angle was ∼106° for 1 whereas for 2 the octahedra were perfectly orthogonal (τ angle of 90°).

The arrangement of the coordination octahedra in compound 2 was due to crystallisation solvent molecules, 2·H2O ·CH3CN, [{MnIJbpy)IJH2O)}IJμ-2,6-Cl2C6H3COO)2IJμ-O){MnIJbpy)-IJNO3)}]NO3·H2O·CH3CN, which propagated the interaction between the monodentate ligands in the two MnIJIII) ions, through a "net" of hydrogen bonds Mn2–LN···W···NO3−···LW–Mn1 (Fig. 3). The interaction between the aqua ligand and nitrate ion was stronger than that of the nitrate ligand and crystallization water (abbreviated as W). The hydrogen-bond distances between the involved oxygen atoms were: dIJO6···O12) = 2.746 Å, dIJO11···O13) = 3.033 Å and dIJO13···O9) = 2.843 Å.

As mentioned above, in this type of compound, it is usual to find hydrogen bonding between the nitrate counteranion and aqua ligand which, in most cases, forms a onedimensional system. However, this is the first compound in which the intramolecular hydrogen bonding between the cationic complex and counteranion generated a cycle, LW···NO3−···W···LN, that blocked any other interaction with neighbour entities.

The nitrate ligand coordinated to the Mn2 ion was perpendicular to the Ot–Mn–OL axis direction, (γ(O9–N5–O7–Mn2) = 91.91°) and the angle between the planes containing the coordinated and non-coordinated nitrate ions was 47.36° (ESI,† Fig. S1). The angle between the two planes containing the hydrogen bonds that generated the extra bridge, O9···O13···O11 and O11···O12···O6 was 59.88° (Fig. 4).

For compound 1, the intermolecular hydrogen bonding between the aqua ligand and perchlorate anion connected two dinuclear entities, LW···ClO4−···LW. (Fig. 5). The OW···OCl distance was slightly different for both perchlorate anions: dIJO6···O12) = 2.874 Å and dIJO6···O14′) = 2.797 Å.

In these types of compounds, the coordination octahedron around the MnIJIII) ions is elongated in the direction of the monodentate ligand, and the Jahn–Teller axes are approximately in the Ot–Mn–OL direction (z axis). Arbitrarily, the x axis could be considered in the Nt–Mn–Ob direction.

Approximate values of the axes length could be obtained by addition of the Mn–L distances of each axis (x = dIJMn–Ob) + dIJMn–Nt), z = dIJMn–OL) + dIJMn–Ot) and y = dIJMn–Oc) + dIJMn–Nc)). For both compounds, the length of x and y axes were similar, whereas some difference was observed in the length of the z axes.

The most significant differences were in the Mn–L distances in the z axes. In both compounds, one site showed a water molecule as a monodentate ligand and the other site the X anion. The Mn–OW distance was similar for both compounds (∼2.23 Å) whereas the Mn–Ot distance (oxygen atom in trans to a

water molecule) was shorter for 1 (2.17 Å) than for 2 (2.22 Å). In the other site, with the X group coordinated to the MnIJIII) ion, the Mn–OCl distance in 1 was ~2.31 Å (there was some delocalization of the perchlorate ligand), whereas the Mn–ON distance in 2 was 2.21 Å. The Mn–Ot distance (oxygen atom trans to the X group) was shorter in 1 (2.13 Å) than in 2 (2.20 Å).

The degree of distortion was evaluated by elongation (Δ) and rhombicity (ρ) parameters, which were calculated using the formulae:3

$$\Delta = \frac{z - \overline{xy}}{\overline{xy}} \text{ and } \rho = \frac{y - x}{x}$$

where $\bar{x}\bar{y}$ = (x + y)/2, Δ represents how different the Jahn–Teller axis is from the average length between x and y axes, and ρ represents distortion within the xy plane. The axis length and distortion parameters for compounds 1 and 2 are shown in Table 3. Interestingly, for compound 1, the most elongated octahedron was that around Mn2 (with the perchlorate ligand) whereas, for compound 2, is was around Mn1 (with the aqua ligand). Surprisingly, the average value for the elongation parameter of both compounds was similar; the obtained value for compound 1 was in the expected range for perchlorate compounds, but it is unusually large for the nitrate compound. The largest Δ value found until now was for an analogous compound with a 3-MeOC6H4CO2 – bridge (12.4) that shows two nitrate ligands.3 Hence, it seems that the unusual hydrogen bond present in compound 2 affected Mn–L distances.

Magnetic properties

Magnetic susceptibility data were recorded for compounds 1 and 2·CH3CN·H2O from room temperature to 2 K (4 K for 2). χMT versus T plots are shown in Fig. 6. At 300 K, the χMT values were lower than expected for two uncoupled MnIJIII) ions (5.6 and 4.5 cm3 mol−1 K for compound 1 and 2, respectively). This fact, together with the decrease in χMT values on cooling, was indicative of a strong antiferromagnetic interaction. This was also clearly evidenced by a maximum in the χM versus T plot, at 26 K for compound 1 and at 90 K for 2, which was indicative of a stronger magnetic interaction in 2 than in 1.

Experimental magnetic susceptibility data were fitted with the PHI program.28 We assumed that the two MnIJIII) ions had the same g value. The best fits of the experimental data corresponded to J = −9.2 cm−1 and g = 2.01, with RIJχMT) = 8.1 × 10−5, RIJχM) = 3.6 × 10−3 for compound 1 and J = −27.3 cm−1 and g = 2.01, with RIJχMT) = 7.1 × 10−5, RIJχM) = 2.0 × 10−3 for compound 2 (considering H = −J·S1·S2 as the spin Hamiltonian).

Magneto-structural correlations

The magnetic coupling constant for perchlorate compounds range between +5.7 cm−1 to −12.6 cm−1, and the result obtained for compound 1 was within this interval. For nitrate compounds, the magnetic coupling constant for compounds reported in the literature range between +11.8 cm−1 to −2.3cm−1. Consequently, the result obtained for compound 2 was out of this range and, moreover, out of the range of perchlorate compounds, being compounds with stronger antiferromagnetic interactions.3

Table S1 in ESI† summarizes the most relevant magnetostructural parameters for the 30 compounds (including 1 and 2) of this type reported until now. Half of them are nitrate compounds (X = NO3) and, between them, 11 compounds show at least one nitrate ion acting as a ligand. Interestingly, three compounds with para susbstituents3,4,8,9 remain nitrate uncoordinated, whereas those with ortho-position nitrate ions are coordinated to one or two MnIJIII) ions. Nevertheless, compounds with meta substituents have a nitrate ion as a counteranion or ligand for 3-Cl10 and 3-MeO,3 respectively, which should be related by the electronic properties of these groups. Table 4 summarizes the magneto-structural parameters for compounds with an ortho mono and disubstituted carboxylate bridge.

n the last years, we have analysed different structural factors affecting the magnetic interaction for compounds with a general formula [{MnIJL)IJNN)}2IJμ-O)IJμ-n-RC6H4COO)2]X2. We found strong influences of the Mn–Ob–Mn angle (α) on the magnetic interaction; major angle values corresponded to greater antiferromagnetic interaction, with a dependence of ∼5 cm− 1 per degree. 4 For this type of compound, the α angle is in the range 121–125° (Table 4 and Table S1 in ESI†). However, other structural parameters enhance the antiferromagnetic interaction: elongation of the coordination octahedra (Δ parameter), relative orthogonal disposition of octahedra, (evaluated as the angle between the Jahn–Teller axes τ(L–Mn···Mn–L)) and the coplanar or perpendicular disposition of the benzylic ring and carboxylate group, □ O C C C carb ar ar □ □ □ □ □ □ .2,3,7

Moreover, as mentioned above, most of the nitrate compounds showed coordination of this anion and a ferromagnetic interaction between MnIJIII) ions. Previously,6 we analysed the influence of the disposition of the nitrate ligand on the magnetic interaction due to their π-acid character. The disposition of the nitrate ligand could be defined by two angles: β(Mn–O–N) and the angle between the planes containing the MnN2O2 fragment and NO3 group (γ) (Fig. 7). When β and γ angles were close to 90° the z2 orbital of the MnIJIII) ion and π*(NO3) were orthogonal and any overlap between them was possible. The best overlap should be achieved for β = 90° and γ = 0°. In this situation, some spin density of the MnIJIII) ion could be delocalized into the nitrate ligand, thereby decreasing the antiferromagnetic interaction.6

Compounds with 3-MeO and with an unsubstituted benzoate bridge showed similar values for these angles (β = 130–134° and γ = 84–88°, see Table S1 in ESI†). Compounds with a substituent on the carboxylate bridge in the ortho position showed a greater range for these angles: β = 118–140° and γ = 30–89°.

Despite of the influence of the different structural parameters on the magnetic interaction, compound 1 followed the expected trends as, for example, the similarity with A and B (Table 4).

The structural parameters of 2 were substantially different from those of compounds with a 2-Cl substituent, J and K, and with most nitrate compounds; their Δ, ω and τ parameters were more similar to those of the perchlorate compounds.

The most relevant differences between compound 1 and 2 were in the τ angle and the presence of the nitrate ligand. The difference in this angle could explain the major antiferromagnetic behaviour of 2. However, the disposition of this ligand, with a small γ angle, suggested some delocalization of the spin density from the z2 orbital of the MnIJIII) ion to the nitrate ligand, which should decrease the antiferromagnetic interaction.

Another factor to take into consideration was the electronic effect of the second chlorine substituent on benzoate bridges. Indeed, 2,6-Cl2C6H3COOH (pKa = 1.59) was more acidic than 2-ClC6H4COOH (pKa = 2.92), indicating a major withdrawing character of the aromatic ring. Previously, we observed that compounds with 2-RC6H4COO− bridges show a weaker antiferromagnetic interaction when R = F (electronwithdrawing group) than when R = Me (electron-donating group).6 In the case reported here, the second chlorine substituent decreased the electronic density on the carboxylate group, and a weaker antiferromagnetic interaction could be expected. However, the experimental data showed an opposite tendency to that expected with regard to electronic factors. Thus, the fact that the structural parameters mentioned above are more relevant became evident. However, the proposed question was if the difference in the τ angle was sufficient to explain the strongest antiferromagnetic interaction on 2.

DFT studies

With the aim of observing the influence of the counteranion on the magnetic properties of these compounds, several calculations were carried out. The coupling constants between transition metals through hydrogen bonding can be theoretically predicted,13 so we attempted to understand the contribution of the bound counteranions. In particular, we were interested in compound 2, for which the unusual hydrogen bonds generated an extra bridge between the MnIJIII) ions (Fig. 3). There were several compounds in which the presence of magnetic interaction through hydrogen bonds could be evidenced.14–26

First, from the crystallographic data we calculated the magnetic interaction in the isolated cationic dinuclear complexes of 1 and 2 ([{MnIJbpy)IJH2O)}IJμ-2,6-Cl2C6H3COO)2IJμ-O){MnIJbpy)IJX)}]+ with X = ClO4− or NO3−, respectively). The results of these calculations suggested that the cationic complex of 1 showed a weaker antiferromagnetic interaction compared with that of the cationic complex of 2 (Tables 5 and 6). This trend was in agreement with the experimental results and confirmed that the structural differences were responsible for the stronger interaction in 2 than in 1. Nevertheless, the second calculation was carried out for the whole compound. In both cases, there were hydrogen bonds

between the dinuclear complex and counteranion but, as mentioned in the structural section, the situation was very different between 1 and 2 and they were analysed separately.

For compound 1, the aqua ligand of two neighbour cationic complexes interacted through a hydrogen bond with two perchlorate counteranions. Hence, in this case, two perchlorate anions acted as extra bridges between two cationic dinuclear complexes of 1, Mn L ClO L Mn W W W W □ □ □ □ □ □ □ 4 2□ . To observe the effect of the extra hydrogen bond bridges, several models based on the structural data of 1 were analysed (Table 5 and Table S2 in ESI†).

The 1A model corresponded to the cationic complex of 1, having only ligand directly bound to manganese atoms. 1B and 1C incorporated only one perchlorate (the two perchlorate counteranions were non-equivalent) together with the cationic complex of 1, interacting with the aqua ligand by hydrogen bonding. Nevertheless, 1D contained two perchlorate anions bound to the cationic complex of 1. The 1E model added a terminal aqua ligand of the neighbouring complex to the 1D one, bound by hydrogen bonds. Finally, the 1⋯1′ model considered the two neighbouring units as a tetranuclear complex (two complexes and two counteranions).

Calculations on the isolated cationic complex of 1 predicted a stronger antiferromagnetic interaction than the experimental one. To analyse the influence of the hydrogen bonds of the aqua ligand with the neighbouring complex, we took the isolated cationic complex of 1 as reference.

Inclusion of a single perchlorate anion (1B and 1C) decreased the antiferromagnetic interaction in the two models. The spin density on the aqua ligand increased while it decreased in the manganese ion with the coordinated water (MnW). This effect was greater when the two anions were present (1D). However, the influence of these hydrogen bonds was negligible on the other manganese ion of the complex (MnCl). The perchlorate anions transferred some electron charge to the aqua ligand, and the latter transferred some electron charge to the manganese ion. Addition of a terminal water molecule did not modify this description significantly.

For the tetranuclear model 1⋯1′, with two cationic complexes interacting through the perchlorate counteranions, the magnitude of the magnetic interaction was intermediate between the models 1E/1D and 1C/1B. The anions transferred now electron charge to the two complexes. The calculations for 1⋯1′ showed negligible magnetic interactions (<10−4cm−1) between the MnIJIII) ions of neighbouring complexes. This was significantly different to the other cases reported in the literature where magnetic interaction between neighbouring entities is present.14–19,21–26 Consequently, the calculation for the isolated cationic complex of 1 indicated a stronger antiferromagnetic interaction that the experimental data. However, when the perchlorate counterions were present, a certain degree of weakening of this interaction was found. Nevertheless, a disagreement between theoretical (1⋯1′) and experimental coupling of only 5 cm−1 was found, probably induced by disorder in the perchlorate anions.

The modification on electronic structure by counteranions is depicted qualitatively in Fig. 8. Perchlorates acted as donors of electron density and transferred it to the aqua ligand, and this was water-bound to the MnIJIII) ion. However, water delocalized mainly β (down) spin density on MnW and

counteracted its α (up) spin density. The final effect was a decrease in spin density on the metal in comparison with the model 1A without counteranions. It is well known that the net magnetic interaction between the MnIIIJ ions is the balance between ferro- and antiferromagnetic contributions. One of the antiferromagnetic contributions involves the z2 orbital of the first center (pointing towards the aqua ligand) and the xz of the second one (in the N2O2 plane). Consequently, the minor spin density on the first metal could diminish the value of this antiferromagnetic contribution.6

In compound 2, there were intramolecular hydrogen bonds between two sites of the cationic complex through one counteranion and one crystallisation water molecule, MnW–LW···NO3−···W···LN–MnN (see the description of the structures section). Hence, in this case, we carried out calculations with the whole compound (2·H2O), including the counteranion and water, and good concordance between experimental and theoretical coupling constants was noted. Alternatively, we considered the isolated cationic complex of 2 by removing both nitrate and water bound by hydrogen bonds to determine the influence of this approach in the magnetic interaction (2A). An extra bridge between the two MnIIIJ ions of the complex decreased the antiferromagnetic interaction (Table 6).

Aiming to understand the effect of this extra bridge, different models were generated from the crystallographic data of 2, by replacing the NO3− anion by neutral and anionic species (X). 2B and 2C corresponded to the models with neutral X groups (MeNO2 and HNO3, respectively) with trisubstituted nitrogen (Table 6 and Table S3 in ESI†). An identical bridging core was present in the 2D model with anionic NO2−, but now disubstituted nitrogen had an electron lone pair. Finally, 2E and 2F containing anionic X groups with carbon as the central atom (HCO3− and MeCO2−, respectively) were considered to evaluate the effect of electronegativity.

The calculated magnetic interaction was dependent on the LN···W···X···LW interaction. The calculated magnetic interaction was similar for models 2A (only the cationic complex), 2B and 2C (neutral X). However, a decrease of ∼13% in the antiferromagnetic interaction was observed when an anionic X species was involved in the hydrogen bond bridge.

Magnetic properties were dependent on the presence of the extra bridge, so we considered the 2A model as the reference. When neutral X groups were incorporated, the main changes in the electronic structure affected both the aqua ligand and molecule that received electron density from a neighbouring neutral molecule and nitrate ligand, respectively. The spin densities on both MnN and MnW atoms decreased slightly, delocalizing it in their ligand, whereas it was zero for bridging water and neutral molecules (as expected for diamagnetic extra bridges). This observation could be explained by redistribution of the spin density from MnN to MnW through the extra bridge (Fig. 9, left). Our calculations revealed that these variations on the spin density of the MnIIIJ ions did not affect the antiferromagnetic interaction. Conversely, in systems with anionic X groups (2, 2E and 2F), the MnN was mostly affected by the extra bridge, which decreased its spin density. The spin density also decreased in the nitrate ligand and increased in the aqua ligand of MnW (Fig. 9, right). Moreover, lower spin densities on MnN and MnW were obtained for models replacing nitrogen by a low electronegative carbon as the central atom in the

X groups (2E vs. 2C, and 2F vs. 2B). Also, new bridging extra ligands had negligible spin density. Consequently, we could associate the decrease in the spin density on manganese atoms with the low antiferromagnetic interaction in these models. As in compound 1, the antiferromagnetic z2/xz contributions decreased due to the lower spin density on the z2 orbital.

A special case was the NO_2^- model (2D), which unexpectedly showed a significant amount of spin density in the extra bridge. Now, the spin density on both manganese ions decreased, especially on MnW, and also on the nitrate ligand, being transferred to the nitrite group and aqua ligand. This could be interpreted as delocalisation of the spin density from MnW, and in minor extension from MnN, to the X group interacting by hydrogen bonds (Fig. 9, bottom).

Then, the effect of the extra bridge between the manganese ions on the dinuclear compound was different depending on the nature of the X group. When X was neutral, electron density was transferred to MnW and to the nitrate ligand (LN), whereas anionic groups transferred it to LW, LN and MnN. Slightly different behaviour was observed for the nitrite group (2D) because it was transferred to LW, MnW and LN.

EXPERIMENTAL

Synthesis

All manipulations were carried out under aerobic conditions. Reagents and solvents were obtained from commercial sources and used without purification. NBu4MnO4 was prepared as described in the literature.29 Caution! Perchlorate salts of compounds containing organic ligands are potentially explosive. Only small quantities of these compounds should be prepared.

[{MnIJbpy)IJH2O)}IJμ-2,6-Cl2C6H3COO)2IJμ-O){MnIJbpy)IJClO4)}] ClO4 (1) MnIJClO4)2·6H2O (0.45 g, 1.25 mmol) was dissolved into 20 mL of MeCN and a solution of 2,6-Cl2C6H3COOH (0.30 g, 1.6 mmol) was added. Then, MeCN solutions of 2,2′-bipyridine (0.0.25 g, 1.6 mmol) and NBu4MnO4 (0.12 g, 0.32 mmol), which had been filtered previously, were added to the abovementioned solution. The resulting solution was stirred for ∼10 min and a first precipitate appeared. The yield was 42.1%. X-ray quality single crystals where obtained by slow diffusion of n-hexane into the mother solution of 1 layered with CH2Cl2 (1 : 1 : 1). Anal. Calcd for C34H24N4O14Cl6Mn2 (M. W. = 1035.2) (%): C, 39.54; H, 2.34; N, 5.43; Cl, 20.33. Found (%): C, 38.91; H, 2.28; N, 5.51; Cl, 20.14.IR (KBr pellet): 3416 (w), 1601 (s), 1572 (m), 1469 (m), 1447 (m), 1429 (s), 1386 (s), 1111 (s), 1084 (s), 770 (s), 728 (m), 626 (m), 499 (m) cm−1.

[{MnIJbpy)IJH2O)}IJμ-2,6-Cl2C6H3COO)2IJμ-O){MnIJbpy)IJNO3)}] NO3·H2O·CH3CN (2·H2O·CH3CN)2,6-Cl2C6H3COOH (0.31 g, 1.6 mmol) in MeCN was added to a solution of MnIJNO3)2·4H2O (0.32 g, 1.25 mmol) in MeCN. Then, previously filtered NBu4MnO4 (0.12 g, 0.32 mmol) dissolved in MeCN was added to the above-mentioned solution. Finally, an MeCN solution of 2,2′-bipyridine (0.25 g, 1.6mmol) was added (total volume, 150 mL), and the resulting solution was stirred for ∼5 min. A brown precipitate appeared from the initial solution. The precipitate was washed with Et2O and dried in air. Dark crystals suitable for X-ray diffraction spectroscopy were obtained by slow evaporation of the mother liquor at room temperature. Yield: 36.9%. Anal. calcd for C34H24N6O12Cl4Mn2·Et2O (M.W. = 1034.4) (%): C, 44.12; H, 3.31; N, 8.12; Cl, 13.71. Found (%): C, 44.03; H, 2.99; N, 8.20; Cl, 13.97. IR (KBr pellet): 3421 (s), 1601 (s), 1497 (m), 1471 (m), 1446 (m), 1445 (w), 1384 (s), 1299 (m), 1171 (w), 1156 (w), 1032 (m), 768 (m), 730 (w), 661 (w), 499 (w).

Physical characterization

Chemical analysis (C, H, N and Cl) was carried out by the Servei de Microanàlisi of the Consell Superior d'Investigacions Científiques. Infrared spectra were recorded on KBr pellets in the 4000–400 cm−1 range with a Termo Nicolet Avatar 330 FT-IR spectrometer. Magnetic susceptibility measurements between 2 and 300 K were carried out in a Quantum Design MPMS XL5 magnetometer at the Unitat de Mesures Magnètiques, Universitat de Barcelona using a field of 300 G. The Pascal constant was used to estimate the diamagnetic corrections for each compound. The fit was undertaken by minimizing the function $R = P[(\chi MT)exp - (\chi MT)calc]2/P[(\chi MT)exp]2$.

X-ray crystallography

The data collection for compound 1 was carried out at 293 K whereas for 2 it was at 100 K, both on a Bruker D8Venture diffractometer equipped with graphite monochromated Mo Kα radiation (λ = 0.71073 Å). Structures were solved and refined using the SHELXL2014 (ref. 30) program. Hydrogen atoms were treated by a mixture of independent and constrained refinement. Crystal data collection and refinement parameters are given in Table S4 in ESI.† For compound 1, the program SQUEEZE31 (part of the PLATON32 package of crystallographic software) was used to calculate the solvent disorder and remove its contribution to the overall intensity data. Twenty-three electrons were found in a 102 Å3 void, which corresponded to the diffuse contribution of an acetonitrile molecule without specific atom positions.

Computational details

Unrestricted density functional calculations were carried out using the Gaussian09 package,33 with the B3LYP hybrid method.34,35 An all-electron triple-ζ basis set was used for all atoms.36 Evaluation of the coupling constants was carried out using high-spin and broken-symmetry states according to non-projected DFT calculations.37 Atomic charges, orbital populations and spin densities were computed by Natural Populations Analysis. These calculations have been used to provide quantitative results,7 including for magnetic coupling towards hydrogen bonds.13

CONCLUSION

The two MnIJIII) dinuclear compounds [{MnIJbpy)IJH2O)}IJμ-2,6-Cl2C6H3COO)2IJμ-O){MnIJbpy)IJX)}]X (X = ClO4 for 1, NO3 for 2) showed different hydrogen bond connectivities, which play important parts on the structural parameters of dinuclear entities. The unusual intramolecular pattern of hydrogen bonds (Mn–LW···X···W···LN–Mn) for 2 could have been responsible for the perfect orthogonality of the coordination octahedral and, indirectly, of the noticeable antiferromagnetic interaction.

Comparison with the analogous compounds with a 2-chlorobenzoate bridge showed that the structural effects of electron-withdrawing chlorine atoms was more important than its electronic factors. DFT studies for both compounds revealed that hydrogen bonds between the counteranion and water molecule decreased the antiferromagnetic interaction. For 1, the intermolecular hydrogen bonds propagated some redistribution of the spin density on the dinuclear complex and modified its magnetic interaction. For 2, the intramolecular hydrogen bonds provided the dinuclear entity with an extra bridge between MnIJIII) ions, and the magnetic interaction weakened the anionic X groups with a major effect observed if the central atom of this group was C instead of N.

CONFLICTS OF INTEREST

There are no conflicts to declare

ACKNOWLEDGEMENTS

This work was supported by the Ministerio de Economia y Competitividad through the projects CTQ 2012-30662, CTQ 2015-64579-C3-1-P and CTQ 2015-63614-P.

REFERENCES

1 J. B. Vincent, H. L. Tsai, A. G. Blackman, S. Wang, P. D. W. Boyd, K. Folting, J. C. Huffman, E. B. Lobkovsky, D. N. Hendrickson and G. Christou, J. Am. Chem. Soc., 1993, 115, 12353–12361.

2 V. Gómez, M. Corbella, O. Roubeau and S. J. Teat, Dalton Trans., 2011, 40, 11968.

3 L. Escriche-Tur, M. Font-Bardia, B. Albela and M. Corbella, Dalton Trans., 2016, 45, 11753–11764.

4 B. Garcia-Cirera, S. Gómez-Coca, M. Font-Bardia, E. Ruiz and M. Corbella, Inorg. Chem., 2017, 56, 8135–8146.

5 M. Corbella, R. Costa, J. Ribas, P. H. Fries, J.-M. Latour, L. Ohrstrom, X. Solans and V. Rodriguez, Inorg. Chem., 1996, 35, 1857–1865.

6 G. Fernández, M. Corbella, G. Aullón, M. A. Maestro and J. Mahía, Eur. J. Inorg. Chem., 2007, 3, 1285–1296.

7 V. Gómez, M. Corbella and G. Aullón, Inorg. Chem., 2010, 49, 1471–1480.

8 M. Corbella, V. Gómez, B. Garcia, E. Rodriguez, B. Albela and M. A. Maestro, Inorg. Chim. Acta, 2011, 376, 456–462.

9 M. Corbella, G. Fernández, P. González, M. Maestro, M. Font-Bardia and H. Stoeckli-Evans, Eur. J. Inorg. Chem., 2012, 2012, 2203–2212.

10 V. Gómez and M. Corbella, Eur. J. Inorg. Chem., 2012, 2012, 3147–3155.

11 L. Escriche-Tur, M. Corbella, M. Font-Bardia, I. Castro, L. Bonneviot and B. Albela, Inorg. Chem., 2015, 54, 10111–10125.

12 C. Chen, H. Zhu, D. Huang, T. Wen, Q. Liu, D. Liao and J. Cui, Inorg. Chim. Acta, 2001, 320, 159–166.

13 C. Desplanches, E. Ruiz, A. Rodríguez-Fortea and S. Alvarez, J. Am. Chem. Soc., 2002, 124, 5197–5205.

14 F. Yoe, M. Flores-Alamo, F. Morales, R. Escudero, H. Cortes-Hernández, M. Castro and N. Barba-Behrens, Inorg. Chim. Acta, 2014, 36–45.

15 K. Roberto, A. Michael and R. Christian, Z. Anorg. Allg. Chem., 2018, 644, 205–214.

16 M. Viciano-Chumillas, M. Gimenez-Marques, S. Tanase, M. Evangelisti, I. Mutikainen, U. Turpeinen, J. M. M. Smits, R. de Gelder, L. J. de Jongh and J. Reedijk, J. Phys. Chem. C, 2008, 112, 20525–20534.

17 R. Fernández de Luis, E. S. Larrea, J. Orive, L. Lezama and M. I. Arriortua, Inorg. Chem., 2016, 55, 11662–11675.

18 A. Yadav, P. Lama, A. Bieńko, D. Bieńko and K. A. Siddiqui, Polyhedron, 2018, 141, 247–261.

19 D. Zhang, H. Wang, Y. Chen, Z. H. Ni, L. Tian and J. Jiang, Inorg. Chem., 2009, 48, 11215–11225.

20 D. Zhang and P. Wang, J. Chem. Crystallogr., 2013, 43, 151–156.

21 I. Nemec, R. Herchel, T. Silha and Z. Travnicek, Dalton Trans., 2014, 43, 15602–15616.

22 R. D. Willett, C. J. Gómez-García, B. Twamley, S. Gómez-Coca and E. Ruiz, Inorg. Chem., 2012, 51, 5487–5493.

23 J. Z. Wu, E. Bouwman, A. M. Mills, A. L. Spek and J. Reedijk, Inorg. Chim. Acta, 2004, 357, 2694–2702.

24 S. Sarkar, A. Datta, A. Mondal, D. Chopra, J. Ribas, K. K. Rajak, S. M. Sairam and S. K. Pati, J. Phys. Chem. B, 2006, 110, 12–15.

25 W. Wernsdorfer, N. Aliaga-Alcalde, D. N. Hendrickson and G. Christou, Nature, 2002, 416, 406–409.

26 J. D. Leng, L. Y. Dian, J. L. Liu and M. L. Tong, Eur. J. Inorg. Chem., 2011, 2317–2326.

27 G. Deacon, Coord. Chem. Rev., 1980, 33, 227–250.

28 N. F. Chilton, R. P. Anderson, L. D. Turner, A. Soncini and K. S. Murray, J. Comput. Chem., 2013, 34, 1164–1175.

29 T. Sala and M. V. Sargent, J. Chem. Soc., Chem. Commun., 1978, 253.

30 G. M. Sheldrick, Acta Crystallogr., Sect. A: Found. Crystallogr. 2008, 64, 112–122.

31 A. L. Spek, Acta Crystallogr., Sect. C: Struct. Chem., 2015, 71, 9–18.

32 A. L. Spek, J. Appl. Crystallogr., 2003, 36, 7–13.

33 M. J. Frisch, et al., Gaussian 09 (Revision B.1), Gaussian Inc., Wallingford, CT, 2010.

34 A. D. Becke, J. Chem. Phys., 1993, 98, 5648–5652.

35 C. Lee, W. Yang and R. G. Parr, Phys. Rev. B: Condens. Matter Mater. Phys., 1988, 37, 785–789.

36 A. Schäfer, H. Horn and R. Ahlrichs, J. Chem. Phys., 1992, 97, 2571–2577.

37 E. Ruiz, J. Cano, S. Alvarez and P. Alemany, J. Comput. Chem., 1999, 20, 1391–1400.

Legends to figures

Figure. 1. Crystal structure of the cationic complex of compound 1 showing the atom labelling scheme. Hydrogen atoms have been omitted for clarity.

Figure. 2 Crystal structures of the cationic complex of compound 2·H2O·CH3CN showing the atom labelling scheme. Hydrogen atoms have been omitted for clarity.

Figure. 3 Hydrogen bonds between both monodentate ligands through the crystallisation water molecule and nitrate counteranion on 2·H2O·CH3CN.

Figure. 4 Planes containing the atoms involved in the hydrogen bonds between LN···W···NO3−···LW for compound 2.

Figure. 5 Hydrogen bonds connecting two dinuclear complexes, through the aqua ligands and perchlorate anions, on compound 1.

Figure. 6 χMT versus T and χM versus T (inset) plots for compounds 1 and 2·H2O·CH3CN. The solid line is the best fit to the experimental data.

Figure. 7 Relative disposition of the nitrate ligand and equatorial plane of the coordination octahedron.

Figure. 8 Main redistribution of the spin density on compound 1 by the presence of hydrogen bonds between the aqua ligands and perchlorate counteranions. Blue arrows represent modifications of the electron density (α (up) and β (down) spin density), while dashed arrows affect mainly α (up) or β (down) spin densities. Local spin for paramagnetic ions are shown in pink.

Figure. 9 Main spin density redistributions due to the hydrogen bonds in the extra bridge for compound 2 and models derived from it. Arrows as Fig. 7.

FIGURE 1

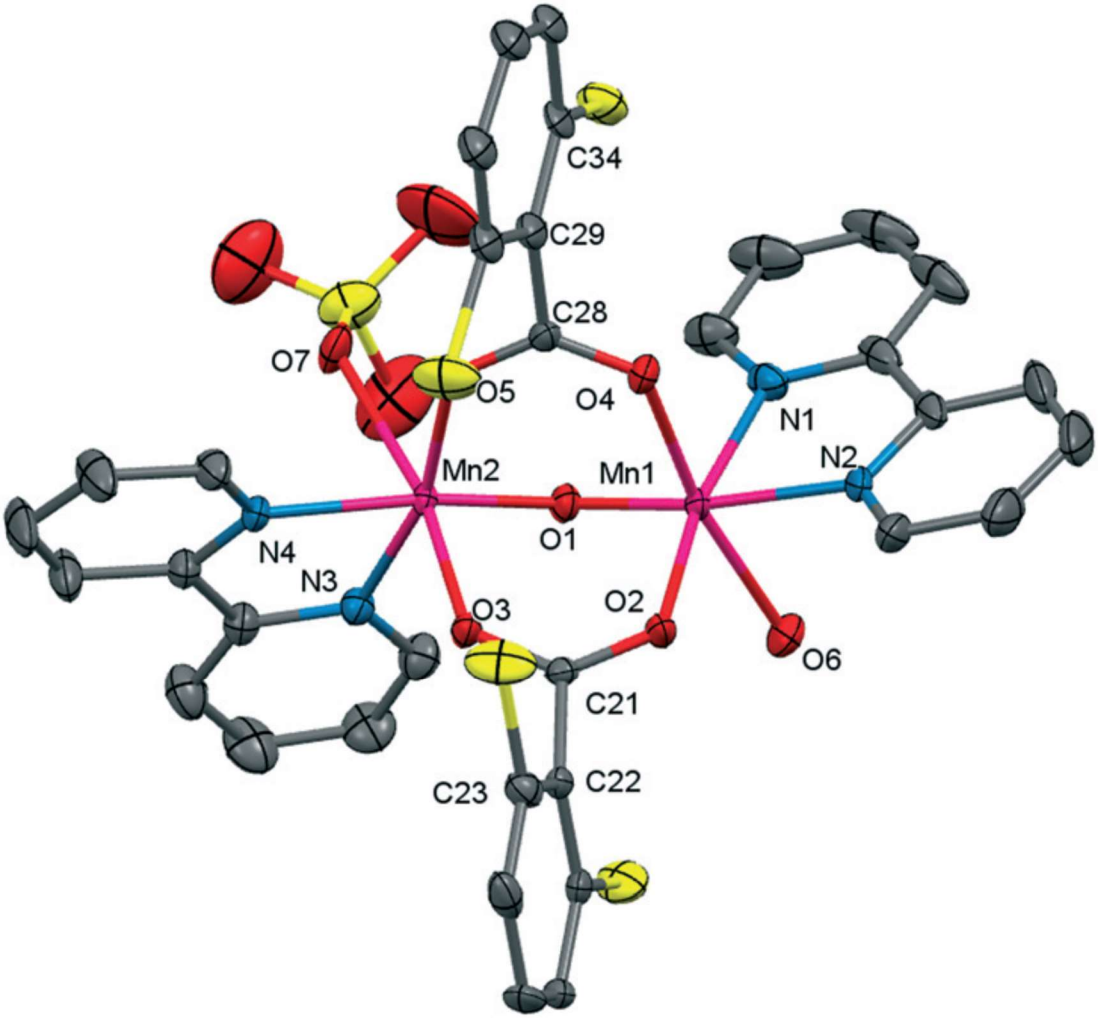

582 **FIGURE 2**

583

584

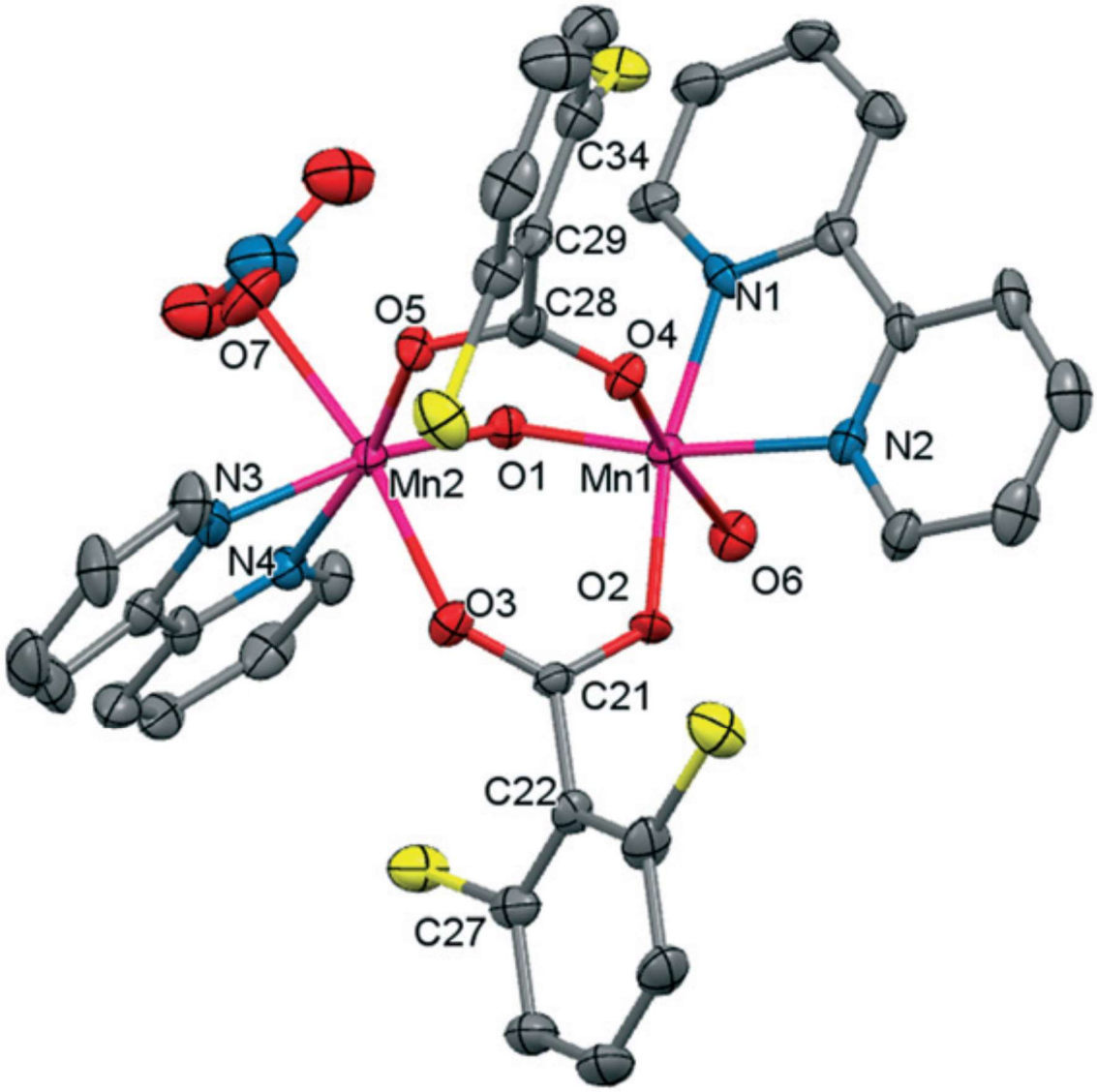

585

586

FIGURE 3

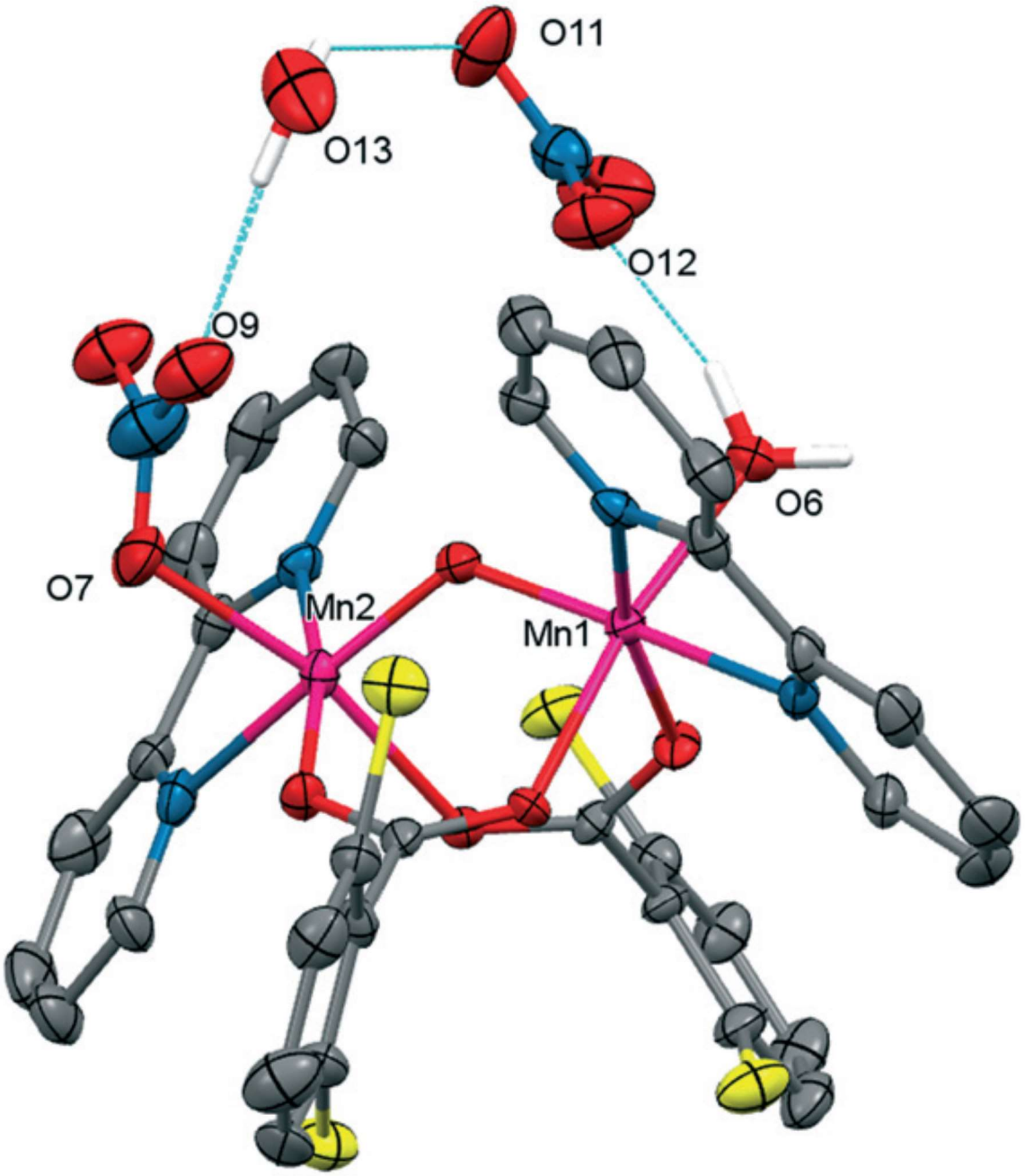

592 **FIGURE 4**

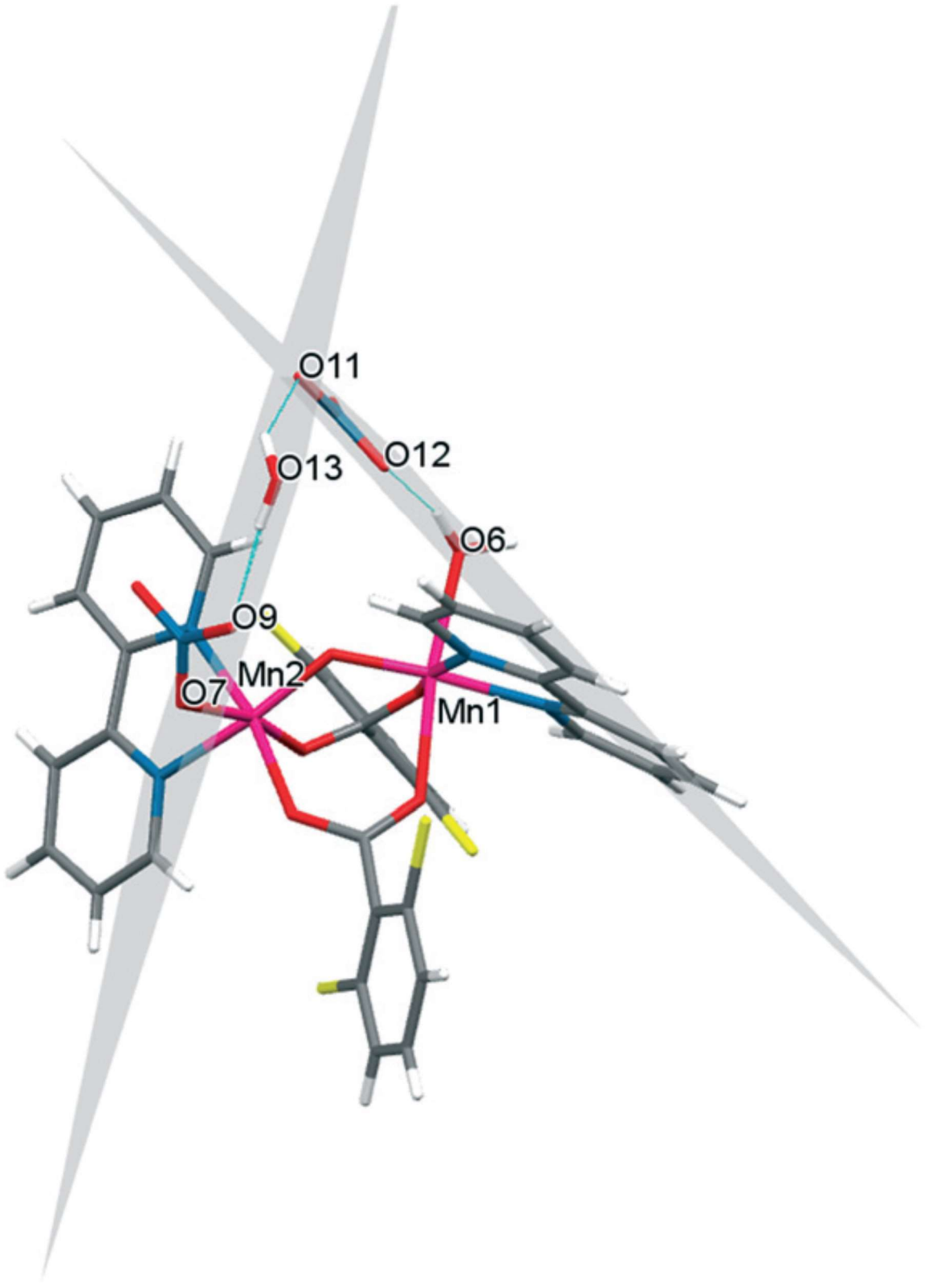

593

594

FIGURE 5.

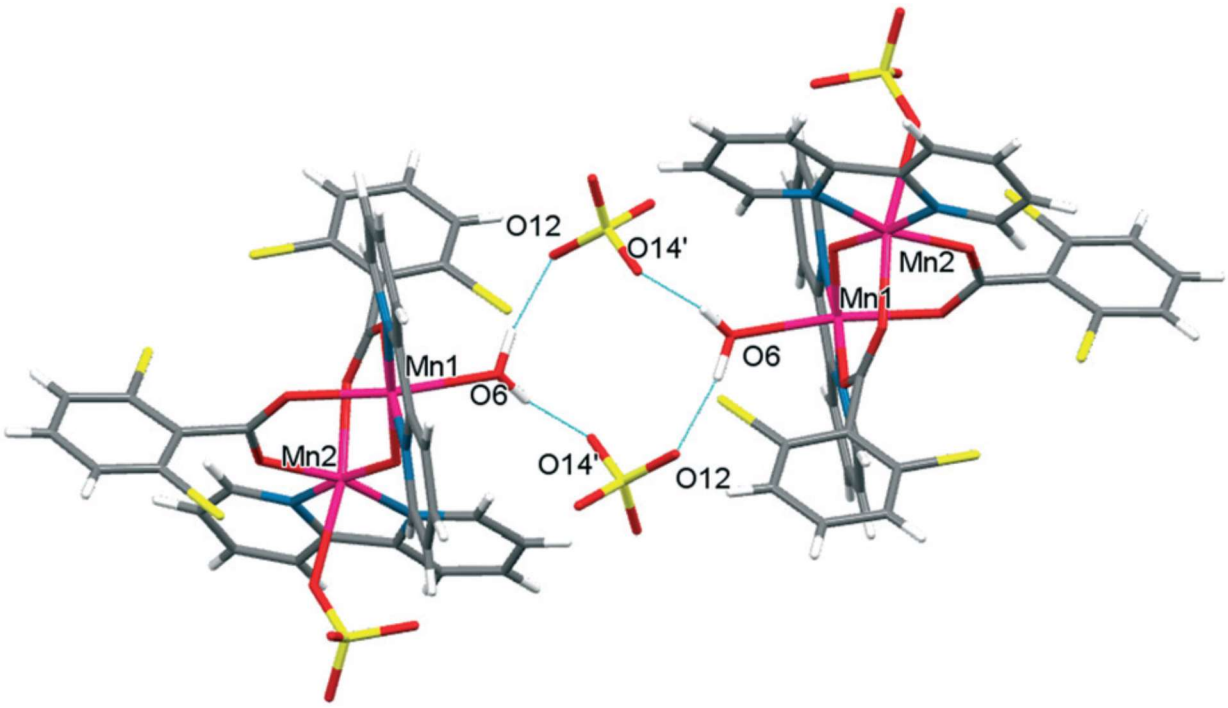

FIGURE 6.

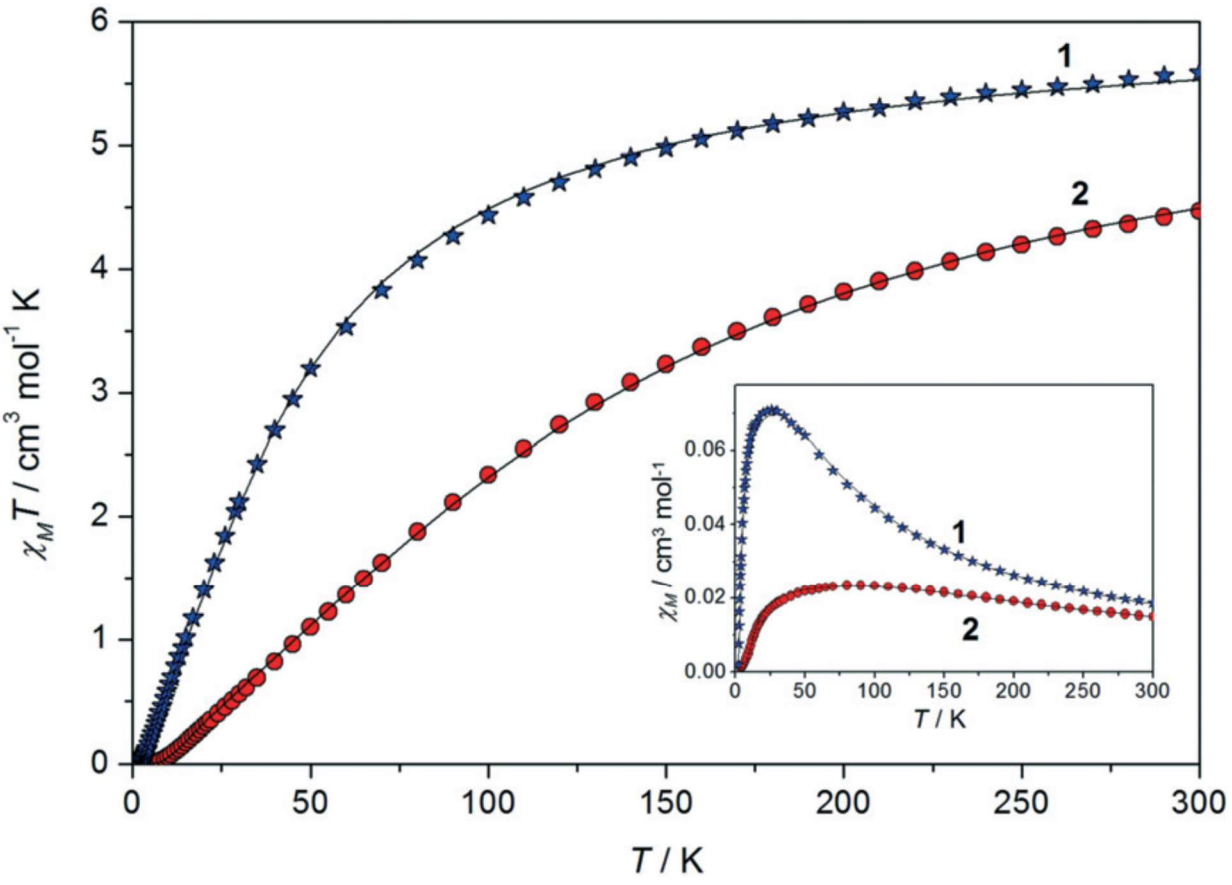

606 **FIGURE 7.**

607

608

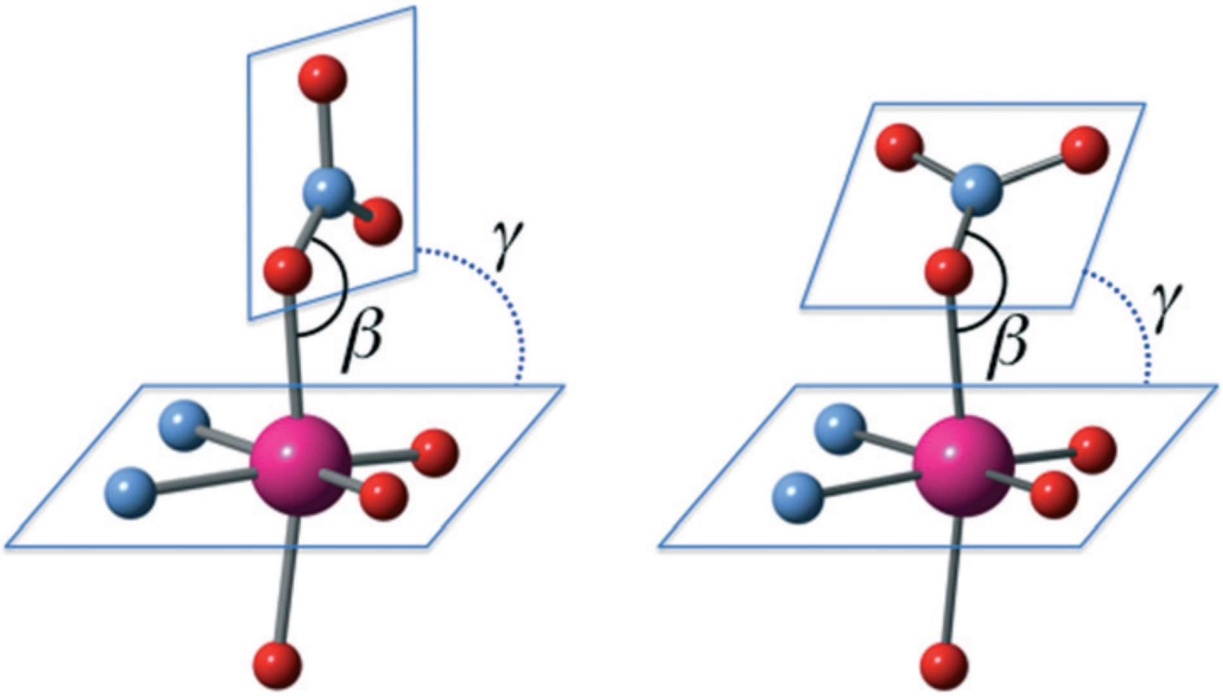

609

610

611

612

613

FIGURE 8.

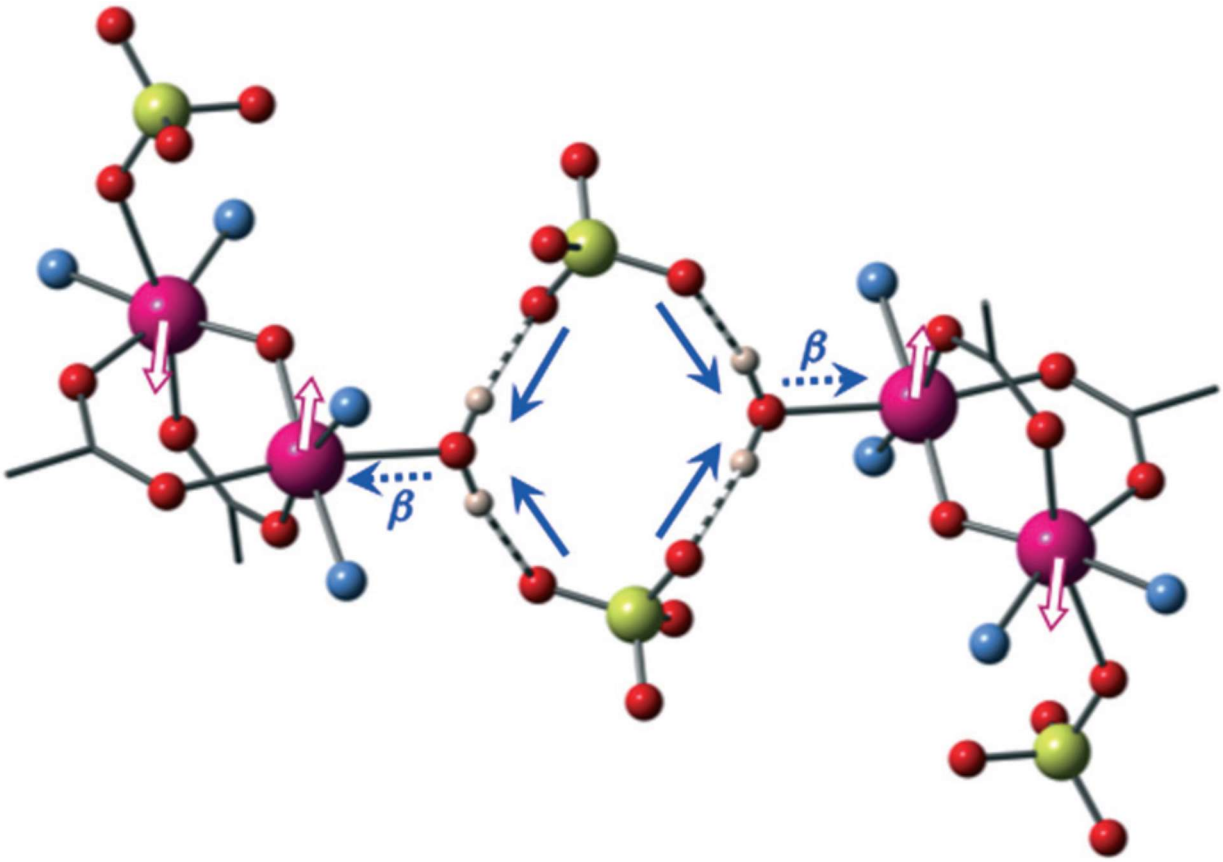

FIGURE 9.

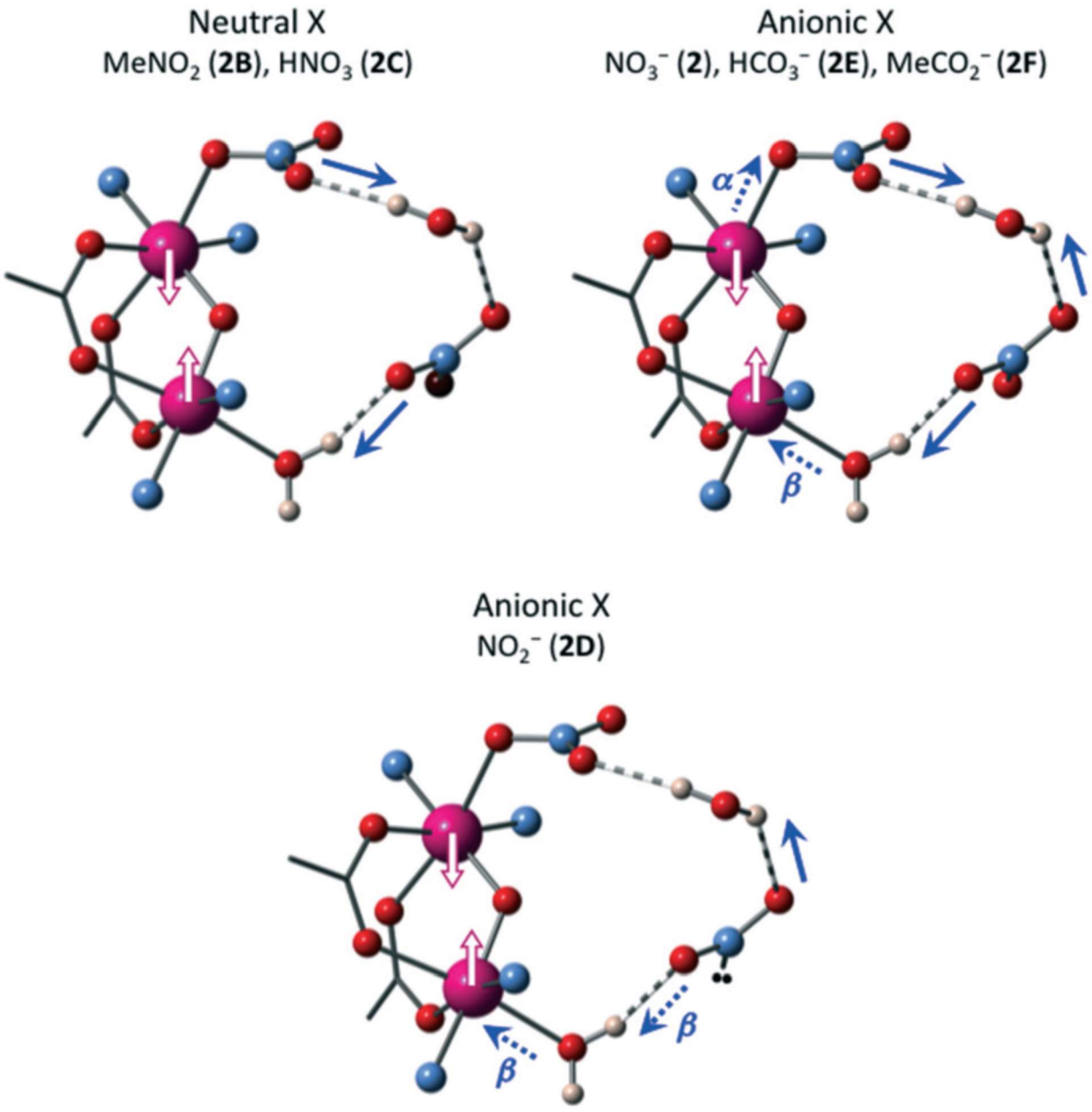
Neutral X
MeNO2 (2B), HNO3 (2C)
Anionic X
NO3− (2), HCO3− (2E), MeCO2− (2F)
α
β
Anionic X
NO2− (2D)
β
β

624 **Table 1** Select interatomic distances (Å) and angles (°) for compound 1

625

Mn1–O1	1.785(2)	Mn2–O1–Mn1	124.4(1)
Mn1–O2	1.972(2)	O1–Mn1–N2	170.13(10)
Mn1–N1	2.052(3)	O2–Mn1–N1	168.99(11)
Mn1–N2	2.058(3)	O4–Mn1–O6	169.22(9)
Mn1–O4	2.166(2)	O1–Mn2–N4	170.56(10)
Mn1–O6	2.238(3)	O3–Mn2–O7	164.4(3)
Mn1···Mn2	3.156(1)	O3–Mn2–O7′	167.4(3)
Mn2–O1	1.783(2)	O5–Mn2–N3	165.45(10)
Mn2–O5	1.964(2)	O6–Mn1–Mn2–O7	104.3(4)
Mn2–N3	2.048(3)	O6–Mn1–Mn2–O7′	107.7(3)
Mn2–N4	2.053(3)	O4–C28–C29–C34	74.6(4)
Mn2–O3	2.131(2)	O3–C21–C22–C23	71.4(5)
Mn2–O7	2.325(12)	Mn1–O4–O5–Mn2	2.4(1)
Mn2–O7′	2.298(13)	Mn1–O2–O3–Mn2	2.1(1)

626

627

628 **Table 2** Select interatomic distances (Å) and angles (°) for compound 2 ·CH3CN·H2O

629

Mn1–O1	1.794(7)	Mn2–O1–Mn1	123.7(4)
Mn1–O2	1.966(7)	O1–Mn1–N2	168.7(3)
Mn1–N1	2.048(9)	O2–Mn1–N1	167.6(3)
Mn1–N2	2.063(8)	O4–Mn1–O6	171.7(2)
Mn1–O4	2.220(6)	O1–Mn2–N3	168.8(3)
Mn1–O6	2.230(7)	O3–Mn2–O7	167.0(3)
Mn1···Mn2	3.162(2)	O5–Mn2–N4	168.8(3)
Mn2–O1	1.792(7)		
Mn2–O5	1.965(7)	O6–Mn1–Mn2–O7	90.0(3)
Mn2–N3	2.062(8)	O4–C28–C29–C34	74.54(8)
Mn2–N4	2.051(8)	O3–C21–C22–C27	75.56(8)
Mn2–O3	2.201(7)	Mn1–O4–O5–Mn2	18.3(3)
Mn2–O7	2.212(8)	Mn1–O2–O3–Mn2	18.8(4)

630

631

632

633

634

635

636 **Table 3** Length of x, y and z axes and elongation (Δ) and rhombicity (ρ) parameters for compounds 1
637 and 2

638

	x (Å)	y (Å)	z (Å)	Δ (%)	ρ (%)
Compound 1					
Mn1 (H_2O)	3.843	4.024	4.404	11.96	4.71
Mn2 (ClO_4)	3.836	4.012	4.443[a]	13.21[a]	4.59
				Av. 12.59	Av. 4.65
Compound 2					
Mn1 (H_2O)	3.857	4.014	4.450	13.07	4.07
Mn2 (NO_3)	3.854	4.016	4.413	12.15	4.20
				Av. 12.61	Av. 4.14

[a] Average values.

639

640

641 **Table 4** Magnetic coupling constants J and selected structural parameters for [{MnIJL)IJNN)}2IJμ-
642 O)IJμ-n-RC6H4COO)2]X2 compounds and [{MnIJL)IJbpy)}2IJμ-O)IJμ-2,6-Cl2C6H3COO)2]X2
643 compounds (1, 2)

644

	Ref.	*n*-R	NN	X	L	J^b/cm^{-1}	α^c/°	Δ^d	ω^e/°	τ^f/°	β^g/°	γ^h/°
2	[a]	2,6-Cl_2	bpy	NO_3	H_2O/NO_3	−27.3	123.7	12.6	75.1	90.0	118	33
A	7	2-Cl	phen	ClO_4	H_2O/H_2O	−12.6	122.9	11.2	77.9	88.3		
B	2	2-Cl	bpy	ClO_4	H_2O/ClO_4[i]	−10.9	122.8	13.3	56.5	92.6		
1	[a]	2,6-Cl_2	bpy	ClO_4	H_2O/ClO_4	−9.2	124.4	12.6	73.0	106.2		
C	6	2-Me	bpy	ClO_4	H_2O/ClO_4	−5.6	122.3	13.8	46.9	101.1		
D	6	2-F	bpy	ClO_4	H_2O/ClO_4	−3.5	124.4	12.7	19.5	93.6		
E	11	2-MeO	bpy	NO_3	H_2O/NO_3	−2.3	123.5	10.8	36.2	78.1	140	87
F	11	2-MeO	bpy	ClO_4	H_2O/ClO_4	−0.7	122.8	12.2	29.2	95.2		
G	6	2-Me	bpy	NO_3	H_2O/NO_3	−0.5	123.1	10.7	28.8	97.2	120	30
H	2	2-Cl	phen	—	NO_3/NO_3	−0.3	124.4	9.7	38.1	101.7	127	47
I	6	2-F	bpy	NO_3	H_2O/NO_3	+1.4	125.1	11.2	18.6	89.2	138	89
J	7	2-Cl	phen	ClO_4	H_2O/H_2O	+2.7	122.9	9.7	46.0	102.0		
K	2	2-Cl	bpy	NO_3	H_2O/NO_3	+3.0	123.0	9.4	25.4	108.5	126	77
L	12	2-COOH	bpy	NO_3	H_2O/NO_3[i]	+4.7	123.5	11.2	19.9	96.4	122	40
M	4	2-Br	phen	NO_3	H_2O/NO_3	+11.8	124.2	−7.7	50.5	96.3	128	69

[a] This work. [b] $H = -J(S_1 \cdot S_2)$. [c] Mn–O–Mn angle. [d] Average elongation: $\Delta = (z - \overline{xy})/\overline{xy}$, $\overline{xy} = (x + y)/2$. [e] Average O–$C_{carb}$–$C_{ar}$–$C'_{ar}$ angle. [f] Relative orientation of the O_b: L–Mn···Mn–L angle. [g] Mn–O–N angle. [h] Angle between the equatorial plane of the octahedra N_2O_2 and NO_3 plane; [i] $3H_2O/1X$; abbreviations: bpy = 2,2′-bipyridine, phen = 1,10-phenantroline.

645

646

647 **Table 5** Calculated magnetic coupling constants and spin density on the MnIJIII) ions and on the aqua

648 ligand for different models based on the crystallographic data of 1 (Mn–LW···IJClO4−)1/2···LW–Mn′).

649 A scheme for framework units in each model is also shown. (H = −JS1·S2)

650

	X	J_{adj}/cm^{-1}	ρ(L_W)/me	ρ(Mn_W)/me	ρ(Mn_{Cl})/me
1A	L_W-none	−19.9	43	3708	−3678
1B	L_W-ClO_4^-	−16.7	53	3694	−3686
1C	L_W-ClO_4^-	−16.5	52	3681	−3692
1D	L_W/$(ClO_4^-)_2$	−13.5	62	3686	−3677
1E	L_W/$(ClO_4^-)_2$-L_W	−13.1	64	3687	−3678
1···1′	L_W/$(ClO_4^-)_2$-L_W	−14.5	58	3686	−3684

651

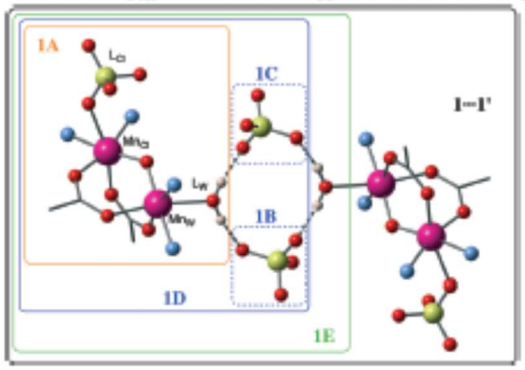

652 **Table 6** Calculated magnetic coupling constants and spin density on the MnIJIII) ions, monodentate
653 ligands, and the extra bridge (crystallization water and counteranion) for 2. A scheme for framework
654 units in each model is also shown (H = −JS1·S2)

655

	X	J_{cal}	ρ(X + W)/me	$\rho(L_{Mn})$/me	$\rho(L_W)$/me	$\rho(Mn_W)$/me	$\rho(Mn_N)$/me
2A	None	−31.3		−96	46	3681	−3678
2B	$MeNO_2$	−31.2	0	−90	48	3690	−3676
2C	$HONO_2$	−31.1	0	−88	50	3689	−3676
2D	NO_2^-	−28.6	67	−90	56	3666	−3674
2	ONO_2^-	−27.6	1	−90	58	3679	−3668
2E	$HOCO_2^-$	−26.5	1	−91	59	3680	−3664
2F	$MeCO_2^-$	−26.3	3	−92	57	3681	−3663

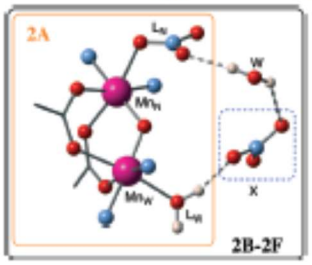

656